Metabolic Engineering 46 (2018) 51–59

Contents lists available at ScienceDirect

Metabolic Engineering

journal homepage: www.elsevier.com/locate/meteng

Engineered cyanobacteria with enhanced growth show increased ethanol production and higher biofuel to biomass ratio

Feiyan Liang, Elias Englund, Pia Lindberg, Peter Lindblad*

Microbial Chemistry, Department of Chemistry-Ångström, Uppsala University, Box 523, SE-751 20 Uppsala, Sweden

ARTICLE INFO

Keywords:
Cyanobacteria
Biofuel
Carbon fixation
Ethanol
RuBisCO
FBP/SBPase
TK
FBA

ABSTRACT

The Calvin-Benson-Bassham (CBB) cycle is the main pathway to fix atmospheric CO_2 and store energy in carbon bonds, forming the precursors of most primary and secondary metabolites necessary for life. Speeding up the CBB cycle theoretically has positive effects on the subsequent growth and/or the end metabolite(s) production. Four CBB cycle enzymes, ribulose-1,5-bisphosphate carboxylase/oxygenase (RuBisCO), fructose-1,6/sedoheptulose-1,7-bisphosphatase (FBP/SBPase), transketolase (TK) and aldolase (FBA) were selected to be co-overexpressed with the ethanol synthesis enzymes pyruvate decarboxylase (PDC) and alcohol dehydrogenase (ADH) in the cyanobacterium *Synechocystis* PCC 6803. An inducible promoter, P*nrsB*, was used to drive PDC and ADH expression. When P*nrsB* was induced and cells were cultivated at 65 μmol photons m^{-2} s^{-1}, the RuBisCO-, FBP/SBPase-, TK-, and FBA-expressing strains produced 55%, 67%, 37% and 69% more ethanol and 7.7%, 15.1%, 8.8% and 10.1% more total biomass (the sum of dry cell weight and ethanol), respectively, compared to the strain only expressing the ethanol biosynthesis pathway. The ethanol to total biomass ratio was also increased in CBB cycle enzymes overexpressing strains. This study experimentally demonstrates that using the cells with enhanced carbon fixation, when the product synthesis pathway is not the main bottleneck, can significantly increase the generation of a product (exemplified with ethanol), which acts as a carbon sink.

1. Introduction

Due to the development of cyanobacterial genetic tools, a large number of carbon-based compounds have been successfully produced directly from CO_2 using sunlight as an energy resource (Lai and Lan, 2015; Miao et al., 2017). Even though there still are challenges to scale up and commercialize these processes, cyanobacteria are regarded as one of the most promising cell-factories to realize sustainable production of alternatives to fossil based compounds. Both abiotic and biotic factors may have effects on the yield and efficiency. Abiotic factors like light intensity, organic carbon source, growth pH, CO_2 concentration and medium composition, have been studied and there are reports that optimizing these factors can indeed increase the production of the specific molecules or products (Gao et al., 2012; Kanno et al., 2017). Regarding biotic factors, genetic engineering and synthetic biology make it possible to change, introduce and alter pathways in the cells. This includes e.g. replacing native enzymes with more efficient alternatives, enzyme optimization, introducing novel, native or synthetic pathways (Erb et al., 2017), engineering regulators and cofactors (Park and Choi, 2017), and engineering photosynthesis and carbon fixation (Li et al., 2017). In many cases, combined optimization of these abiotic and biotic factors results in higher yield.

Among all the strategies, increasing carbon fixation theoretically increases the amount of carbon available in the cells for the formation of desired product(s). The Calvin-Benson-Bassham (CBB) cycle is the primary carbon fixation pathway in nature (Fig. 1). However, it uses one of the most inefficient enzymes, ribulose-1,5-bisphosphate carboxylase/oxygenase (RuBisCO), to carboxylate ribulose-1,5-bisphosphate (RuBP) with one molecule of CO_2 to form two molecules of 3-phosphoglycerate. The trade-off between CO_2 affinity and carboxylation rate makes it challenging to further improve the performance of RuBisCO (Greene et al., 2007; Savir et al., 2010). Since RuBisCOs from cyanobacteria tend to have a faster carboxylation rate compared to higher plant RuBisCOs (Savir et al., 2010), transforming cyanobacterial RuBisCOs into higher plants attracts researchers who are putting efforts on increasing crop yield. There is a report on successful introduction of a functional RuBisCO from cyanobacterium *Synechococcus elongatus* PCC 7942 into tobacco, with increased CO_2 fixation rate per unit of enzyme in the engineered lines. However, the transformant line could only grow autotrophically under elevated CO_2 concentration (3% v/v CO_2/air) (Lin et al., 2014; Occhialini et al., 2016). Co-overexpressing RuBisCO biogenesis chaperones is another strategy that has been shown

* Corresponding author.
E-mail address: Peter.lindblad@kemi.uu.se (P. Lindblad).

https://doi.org/10.1016/j.ymben.2018.02.006
Received 10 November 2017; Received in revised form 14 December 2017; Accepted 18 February 2018
Available online 23 February 2018

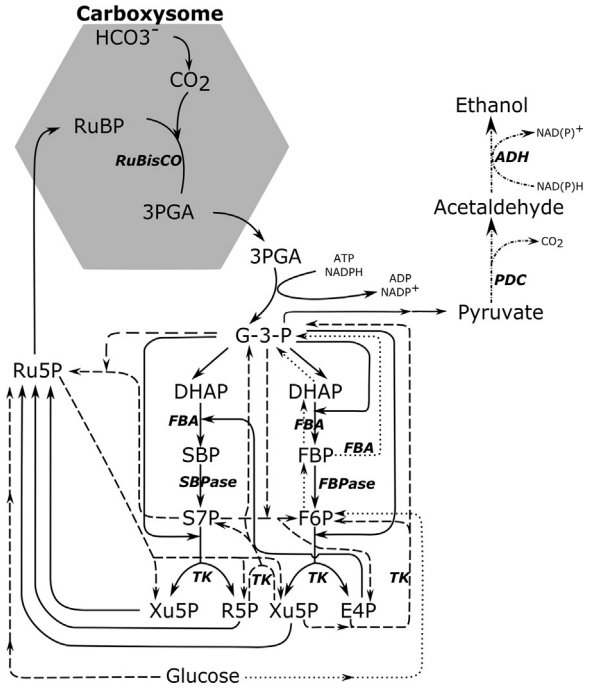

Fig. 1. The Calvin-Benson-Bassham cycle (solid lines), the oxidative pentose phosphate pathway (dashed lines), the glycolysis pathway (dotted lines) in cyanobacteria and the ethanol synthetic pathway (dash-dot lines). The enzymes overexpressed in this study were written in bold italic form. Abbreviations of intermediates: RuBP, ribulose-1,5-bisphosphate; 3PGA, 3-phosphoglycerate; G-3-P, glyceraldehyde-3-phosphate; DHAP, dihydroxyacetone phosphate; FBP, fructose-1,6-bisphosphate; SBP, sedoheptulose-1,7-bisphosphate; F6P, fructose-6-phosphate; S7P, sedoheptulose-7-phosphate; E4P, erythrose-4-phosphate; Xu5P, xylulose-5-phosphate; R5P, ribose-5-phosphate; Ru5P, ribulose-5-phosphate. Abbreviations of enzymes: RuBisCO, Ribulose-1,5-bisphosphate carboxylase/oxygenase; FBA, aldolase; FBP/SBPase, fructose-1,6-/sedoheptulose-1,7-bisphosphatase; TK, transketolase; PDC, pyruvate decarboxylase; ADH, acetaldehyde dehydrogenase. Modified from Liang and Lindblad (2016).

to benefit photosynthesis and tobacco growth (Whitney et al., 2015). In cyanobacteria, several studies have demonstrated increased photosynthesis (Iwaki et al., 2006) and product formation by RuBisCO engineering. Regarding product formation, increased isobutyraldehyde in *Synechococcus elongatus* PCC 7942 with additional RuBisCO genes from *Synechocccus elongatus* PCC 6301 and increased fatty acid in *Synechococcus* PCC 7002 with *Synechoccus elongatus* PCC 7942 RuBisCO genes heterologously expressed were reported (Atsumi et al., 2009; Ruffing, 2014).

Several other enzymes in the CBB cycle, fructose-1,6/sedoheptulose-1,7-bisphosphatase (FBP/SBPase), aldolase (FBA) and transketolase (TK), are targets to increase photosynthesis, carbon fixation, and/or biomass accumulation in cyanobacteria or plants (Liang and Lindblad, 2016; Raines, 2003; Zhu et al., 2007). In plants, one of the four enzymes may have the main control of the carbon flux under a specific growth condition (Raines, 2003; Zhu et al., 2007). Systematic studies using cyanobacteria are limited. Overexpressing chloroplast FBPase, whose function is carried out by FBP/SBPase in cyanobacteria, resulted in varied effects in different host organisms, depending on growth conditions (Dejtisakdi and Miller, 2016; Ma et al., 2005). In addition, overexpressing SBPase, another function of FBP/SBPase in cyanobacteria, had a positive effect on initial RuBisCO activity, probably by increasing the RuBP concentration or by keeping RuBisCO activase in the soluble stroma in plants (Feng et al., 2007; Miyagawa et al., 2001). This clearly indicates interactions of regulation between enzymes in the CBB cycle. The effects of overexpressing SBPase, or the bifunctional protein FBP/SBPase, on the formation of desired products have been intensively studied in plants (Köhler et al., 2017; Ogawa et al., 2015; Rosenthal et al., 2011; Simkin et al., 2017). The other two enzymes, TK and FBA, have relatively less reports. To our knowledge, there are no reports of TK engineering to enhance generation of desired compounds. However, there is one report that overexpressing TK in tobacco had severe effects on growth, which were related to thiamine homeostasis (Khozaei et al., 2015). Furthermore, in TK antisense plants a small decrease in the levels of this enzyme resulted in a significant decrease in photosynthesis (Henkes et al., 2001). Some promising results showed that overexpressing FBA, homogeneously or heterogeneously, resulted in increased CO_2 fixation efficiency in *Arabidopsis thaliana* (Simkin et al., 2017; Uematsu et al., 2012).

Despite the limitations of the CBB cycle, the carbon sink itself may be another limitation. Enhancing the sucrose export enhanced the quantum efficiency of PSII in *Synechococcus elongatus PCC* 7942 without any modification on the CBB cycle or light reactions (Abramson et al., 2016). Considering using organisms with larger sink capacity, introducing functional RuBisCO, even a functional CBB cycle, into heterotrophic organisms like *Escherichia coli* (*E. coli*) and yeast (Antonovsky et al., 2016, 2017) is another direction of carbon fixation research. Obtained strains could not grow only with atmospheric CO_2 since they do not photosynthesize. However, with laboratory evolution, *E. coli* with RuBisCO and phosphoribulokinase could synthesize sugar with a concomitant consumption of pyruvate (Antonovsky et al., 2017). This engineering allowed the cells to reuse CO_2 released from glycolysis and thus increase the formation of desired products (Li et al., 2017).

In our earlier studies, we demonstrated that overexpressing four selected CBB cycle enzymes individually resulted in increased growth under certain growth conditions (Liang and Lindblad, 2016, 2017). To investigate the potential of these strains for enhancing productivity, we combined the engineered strains exhibiting increased growth with an introduced capacity to produce ethanol, allowing us to address the question whether the increased productivity resulting from CBB cycle enzyme overexpression can be utilized to enhance generation of a selected carbon-based product.

2. Materials and methods

2.1. Escherichia coli and Synechocystis PCC 6803 cultivation

E. coli was cultivated with LB in liquid or on 1.5% agar (w/v) plates under 37 °C. *Synechocystis* PCC 6803 (*Synechocystis* hereafter) was cultivated with BG11 (Stanier et al., 1971) in liquid or on 1.5% agar (w/v) plates at 30 °C. 50 μg/ml kanamycin was used for selection in both *E. coli* and *Synechocystis*. For ethanol measurements, cells were cultivated with the addition of 25 μg/ml kanamycin.

Two different systems were used to cultivate *Synechocystis* ethanol-producing strains. One was in 6-well TC plate (Sarstedt) with 4 ml BG11 and 25 μg/ml kanamycin under a light intensity of 15 μmol photons m^{-2} s^{-1}. The second system was in Biolite flasks (Plug seal, Thermo Scientific) with 10 ml BG11, 25 μg/ml kanamycin, 50 mM $NaHCO_3$ and 40 mM HEPES-NaOH (pH 7.5) under 65 μmol photons m^{-2} s^{-1}. On days 3 and 5, $NaHCO_3$ was added to a final concentration of 50 mM. The Biolite flask system was used to prevent the evaporation of ethanol under relatively higher light intensity. 2.5 μM Ni^{2+} ($NiCl_2$) was used to induce P*nrsB* when induction was required.

2.2. Plasmids construction and conjugation into Synechocystis

All genetic constructs were based on pPMQAK1 (Huang et al., 2010), and the genetic material inserted between the restriction sites *EcoRI* and *SpeI* or *PstI*. All restriction enzymes were from Thermo Fisher Scientific. Table 1 shows the plasmids used in this study, graphically presented in Fig. 2. *Synechocystis* engineered strains with specific plasmid conjugated were named after the conjugated plasmids.

Plasmids were transferred to *Synechocystis* by conjugation, as described before (Liang and Lindblad, 2016). The pPMQAK1 has an RSF1010-derived replicon with a copy number of about 10–29 per cell

Table 1
Plasmids and *Synechocystis* PCC 6803 (*Synechocystis*) engineered strains constructed in this study.

Plasmid	Promoter(s) and enzyme(s)	*Synechocystis* strains
control	(Liang and Lindblad, 2016)	control
pEtOH	P*nrsB*, pyruvate decarboxylase (PDC) and alcohol dehydrogenase (ADH) (Englund et al., 2016)	EtOH
pEtOH-rbcSC	P*nrsB*, PDC and ADH; P*psbA2*, small subunit tagged (FLAG) RuBisCO	EtOH-rbcSC
pEtOH-70glpX	P*nrsB*, PDC and ADH; P*psbA2*, FBP/SBPase from *Synechococcus* PCC 7002	EtOH-70glpX
pEtOH-tktA	P*nrsB*, PDC and ADH; P*psbA2*, TK	EtOH-tktA
pEtOH-fbaA	P*nrsB*, PDC and ADH; P*psbA2*, FBA	EtOH-fbaA

in *Synechocystis* (Marraccini et al., 1993; Ng et al., 2000).

2.3. Semi-quantitative PCR (RT-PCR) and Western-immunoblotting

RT-PCR and Western-immunoblotting were performed as detailed before (Liang and Lindblad, 2016). Pyruvate decarboxylase antibody was kindly provided by Dr. Lonnie Ingram (University of Florida, USA, Aldrich et al., 1992). One-way ANOVA was used for statistical analyses.

2.4. Ethanol and dry cell weight (DCW) measurements

Ethanol was quantified as previously described (Englund et al., 2016). At the same time point as ethanol measurements, dry cell weight (DCW) was determined. 13 ml cultivation tubes (Sarstedt) were pre-dried at 70 °C oven for 12 h. Cells were harvested by centrifugation at 5000 rpm for 20 min, and dried at 70 °C oven for 24 h before measuring the DCW. One-way ANOVA was used for statistical analyses.

3. Results

3.1. Enhanced ethanol production in cyanobacterial cells grown at 65 μmol protons m^{-2} s^{-1}

An ethanol synthesis pathway, consisting of pyruvate decarboxylase (encoded by *pdc* from *Zymomonas mobilis*, PDC) and alcohol dehydrogenase (*slr1192* from *Synechocystis*, ADH) was introduced into wild type *Synechocystis* as an operon driven by the inducible promoter P*nrsB* (Englund et al., 2016) on the RSF1010 based shuttle vector pPMQAK1 (Huang et al., 2010). The plasmid was further engineered to include genes encoding one of four selected enzymes, RuBisCO and FBP/SBPase (the SBPase function), specific for the CBB cycle, and TK and FBA, present in both the CBB cycle and the oxidative pentose phosphate (OPP) or the glycolysis pathway. The FBPase function of FBP/SBPase also catalyzes reactions in gluconeogenesis (Tamoi et al., 1999). These four enzymes were individually cloned in the opposite direction to the ethanol synthesis operon, with expression from the native *psbA2* promoter (Liang and Lindblad, 2016; Englund et al., 2016), and introduced into *Synechocystis* cells (see Fig. 2 and Table 1 for plasmid constructs and resulting strains). P*nrsB* is induced by Ni^{2+}, but still has a weak expression without induction in cells grown in BG11-medium (Englund et al., 2016). This may due to leakiness of P*nrsB* and the presence of trace amount of Co^{2+}, which is another inducer of P*nrsB*, in the BG11 medium (Englund et al., 2016). Ethanol production was detected both with and without induction of P*nrsB*.

When strains were cultivated with $NaHCO_3$ and Ni^{2+} induction, the control (wild type with empty vector) strain, without ethanol production cassette, grew best, while the EtOH strain, expressing PDC and ADH alone (Table 1), grew the second best (Fig. 3A). Without Ni^{2+} induction, the EtOH strain still grew faster than any of the strains with one of the four selected CBB cycle genes co-overexpressed at the early stage of cultivation. However, the EtOH strain stopped growing after day 3, and thereafter exhibited a slowly declining OD_{750}, while the other strains kept growing (Fig. 3B).

The ethanol production patterns of ethanol-producing strains with or without induction of P*nrsB* were very different. When P*nrsB* was induced, all four strains co-expressing CBB cycle enzymes with the ethanol synthesis cassette produced more ethanol than the reference strain EtOH. At the end of the cultivation period, ethanol production in EtOH-rbcSC, EtOH-70glpX, EtOH-tktA and EtOH-fbaA was increased by 55%, 67%, 37% and 69%, respectively, compared to the EtOH strain (Fig. 3C). In contrast, the ethanol production pattern was opposite when P*nrsB* was not induced. Ethanol yields in the strains co-overexpressing one of the four selected CBB cycle genes were much lower, reaching only around 2% of the ethanol production of the EtOH strain (Fig. 3D). Besides, ethanol production without induction was much lower than that with induction in general, which was expected since there was dramatic difference on the strength of P*nrsB* with and without induction (Englund et al., 2016). For example, the ethanol level of strain EtOH without induction only reached 39.4% of that with induction on day 3 (Fig. 3D).

To compare the abilities of different strains to convert atmospheric CO_2 into organic carbon compounds (except for ethanol), dry cell weight (DCW) was measured. When cells were cultivated with Ni^{2+} added, at the early growth stage, ethanol production had severe effects on DCW. The DCW of EtOH, EtOH-rbcSC, EtOH-70glpX, EtOH-tktA and EtOH-fbaA were significantly lower than that in the control strain,

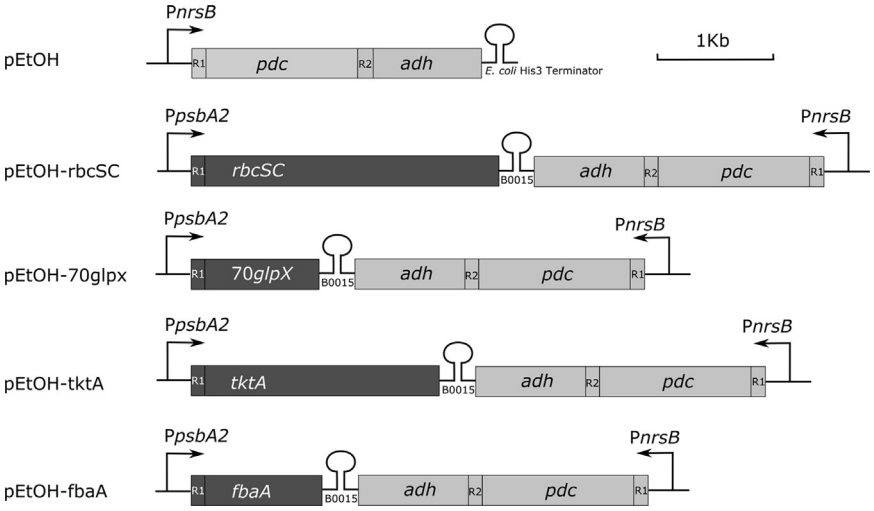

Fig. 2. Plasmid constructs. *pdc*, pyruvate decarboxylase gene from *Zymononas mobilis*; *adh*, *slr1192* from *Synechocystis* PCC 6803; *rbcSC, slr0009-slr0011-slr0012-FLAG* with RuBisCO-encoding genes from *Synechocystis* PCC 6803 (Liang and Lindblad, 2017); *70glpX*, *SYNPCC7002_A1301* from *Synechococcus* PCC 7002; *tktA*, *sll1070* from *Synechocystis* PCC 6803; *fbaA*, *sll0018* from *Synechocystis* PCC 6803. P*psbA2* and P*nrsB* represents promoters (Liang and Lindblad, 2016; Englund et al., 2016). R represents ribosome binding site.

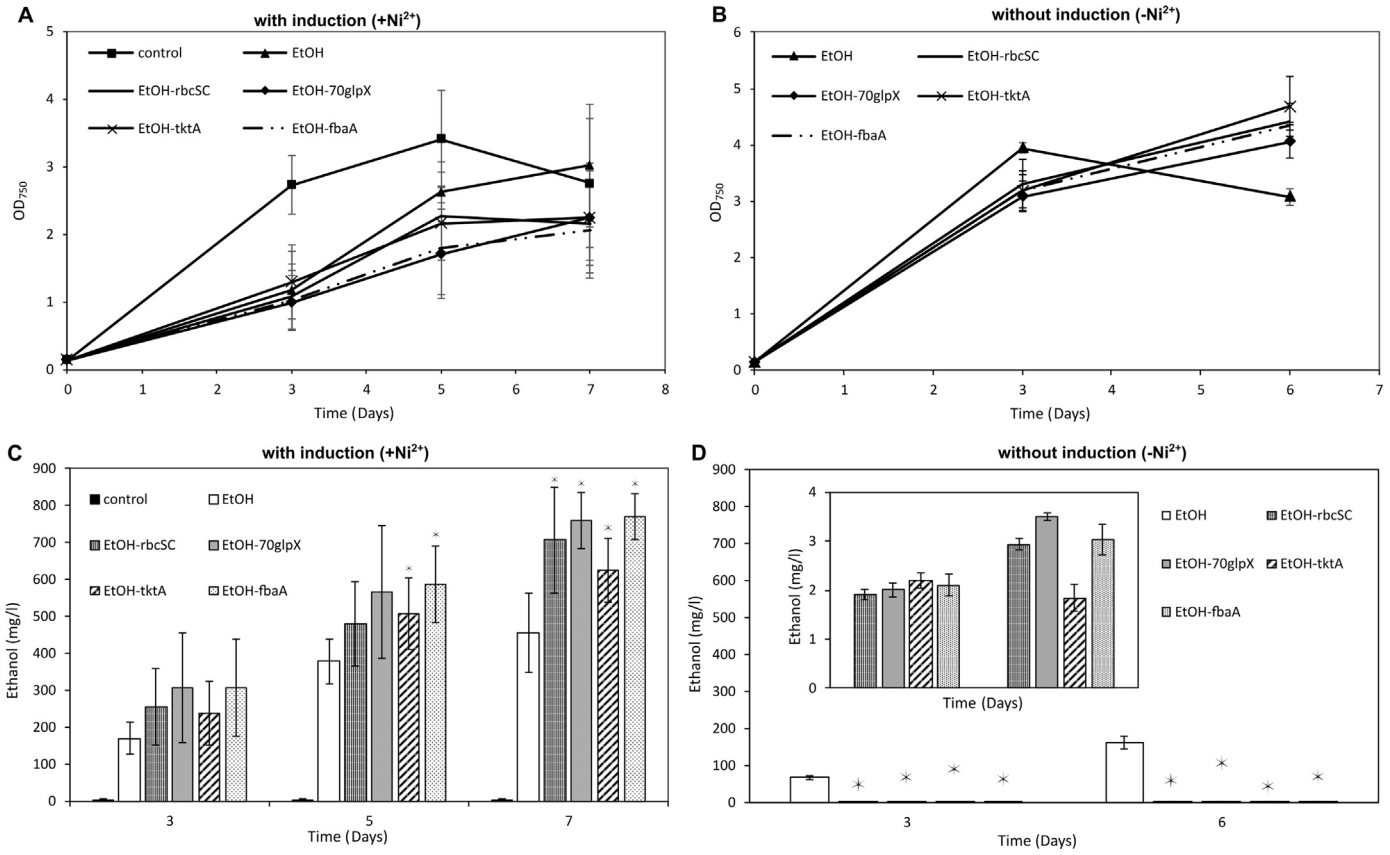

Fig. 3. Growth curves (A and B) and ethanol yield (C and D) of *Synechocystis* PCC 6803 strains, the empty vector control strain (in A and C), EtOH, EtOH-rbcSC, EtOH-70glpX, EtOH-tktA and EtOH-fbaA. Cells were cultivated with 50 mM $NaHCO_3$ under 65 µmol protons m^{-2} s^{-1} light intensity with (A and C) and without (B and D) 2.5 µM Ni^{2+} induction. Error bars represent standard deviations from six biological replicates conducted in three independent experiments (A and C) and from biological triplicates (B and D). In figures C and D, one-way ANOVA analysis was applied. Asterisks indicate a significant difference ($P < 0.05$) between strains with the ethanol synthesis pathway alone and with one of the CBB genes co-overexpressed. The insert in figure D indicated higher resolution. For strain information see Table 1.

without ethanol synthesis cassette. On the third day of cultivation, the DCW of the EtOH strain was the lowest. At the end, the difference had diminished but the DCW of the control remained slightly higher than that in all the other strains (Fig. 4A).

The DCW and ethanol yield together represents the total carbon output (total biomass) of the cultures. Similar to the DCW, at the early growth stage, the total biomass of ethanol-producing strains was less than that in the control strain, while the total biomass of the EtOH strain was significantly lower and the other four strains with one of the CBB cycle genes co-overexpressed had similar total biomass as the control strain (Fig. 4B). This resulted in 33%, 39%, 38% and 34% more total biomass of EtOH-rbcSC, EtOH-70glpX, EtOH-tktA and EtOH-fbaA compared to that in the EtOH strain on day 3. During the cultivation period, the ethanol producing strains accumulated more total biomass than the control strain, mainly in the form of ethanol. On the last day of cultivation, ethanol producing strains had generated 38.8%, 49.4%, 59.7%, 51%, and 52.9% more total biomass than the control strain (Fig. 4B). At the same time, EtOH-rbcSC, EtOH-70glpX, EtOH-tktA and EtOH-fbaA accumulated 7.7%, 15.1%, 8.8% and 10.1% more total biomass compared to the EtOH strain (Fig. 4B). Cells only containing the ethanol synthesis cassette (EtOH) produced 30.2% of the total biomass in the form of ethanol, while the strains with one of the four-selected genes co-overexpressed with the ethanol synthesis genes increased the ethanol to total biomass ratio to 43.6% (EtOH-rbcSC), 45.2% (EtOH-70glpX), 38.4% (EtOH-tktA) and 47.4% (EtOH-fbaA) (Fig. 4C).

The same results were not observed when using cells cultivated without P*nrsB* being induced. Strains with the CBB genes co-overexpressed with ethanol synthesis genes had only slightly higher DCW than the EtOH strain (Fig. 4D) while the total biomass (ethanol plus DCW) was slight lower (Fig. 4E), even though neither effect was statistically significant. The ethanol to total biomass ratio was much lower in EtOH-rbcSC, EtOH-70glpX, EtOH-tktA and EtOH-fbaA (less than 0.3%) than in the EtOH strain (13.3%, Fig. 4F). This is an opposite pattern compared to that in cells cultivated with P*nrsB* induced.

3.2. PDC levels determined by cell physiology

The ethanol production pattern with and without Ni^{2+} induction was dramatically different between strains EtOH, EtOH-rbcSC, EtOH-70glpX, EtOH-tktA and EtOH-fbaA (Fig. 3C and D). In order to determine whether PDC protein levels differ between these strains, cells with and without induction were examined. With P*nrsB* induced, PDC was expressed as demonstrated by clear PDC bands on SDS-PAGE gels and corresponding Western immunoblotting using specific anti-PDC antibodies (Fig. 5A). Quantity analysis of PDC content on Western immunoblotting showed that EtOH-rbcSC, EtOH-70glpX, EtOH-tktA and EtOH-fbaA had more PDC protein compared to the EtOH strain (Fig. 5B), which is in agreement with the observed levels of ethanol (Fig. 3C). Without P*nrsB* induced, PDC could not be detected on SDS-PAGE, and only PDC from EtOH strain could be detected on the Western immunoblotting membrane (Fig. 5A), which is again consistent with observed ethanol production (Fig. 3D). In EtOH-tktA, the TK band was also clearly detected on SDS-PAGE gels (Fig. 5A), in cells both with and without induction. This showed the shuttle vector was not lost.

Using semi-quantitative RT-PCR, we could demonstrate that *pdc* was transcribed in strains with induction, since *pdc* mRNA could be detected after 24 cycles, with 500 ng total RNA as starting material for the cDNA

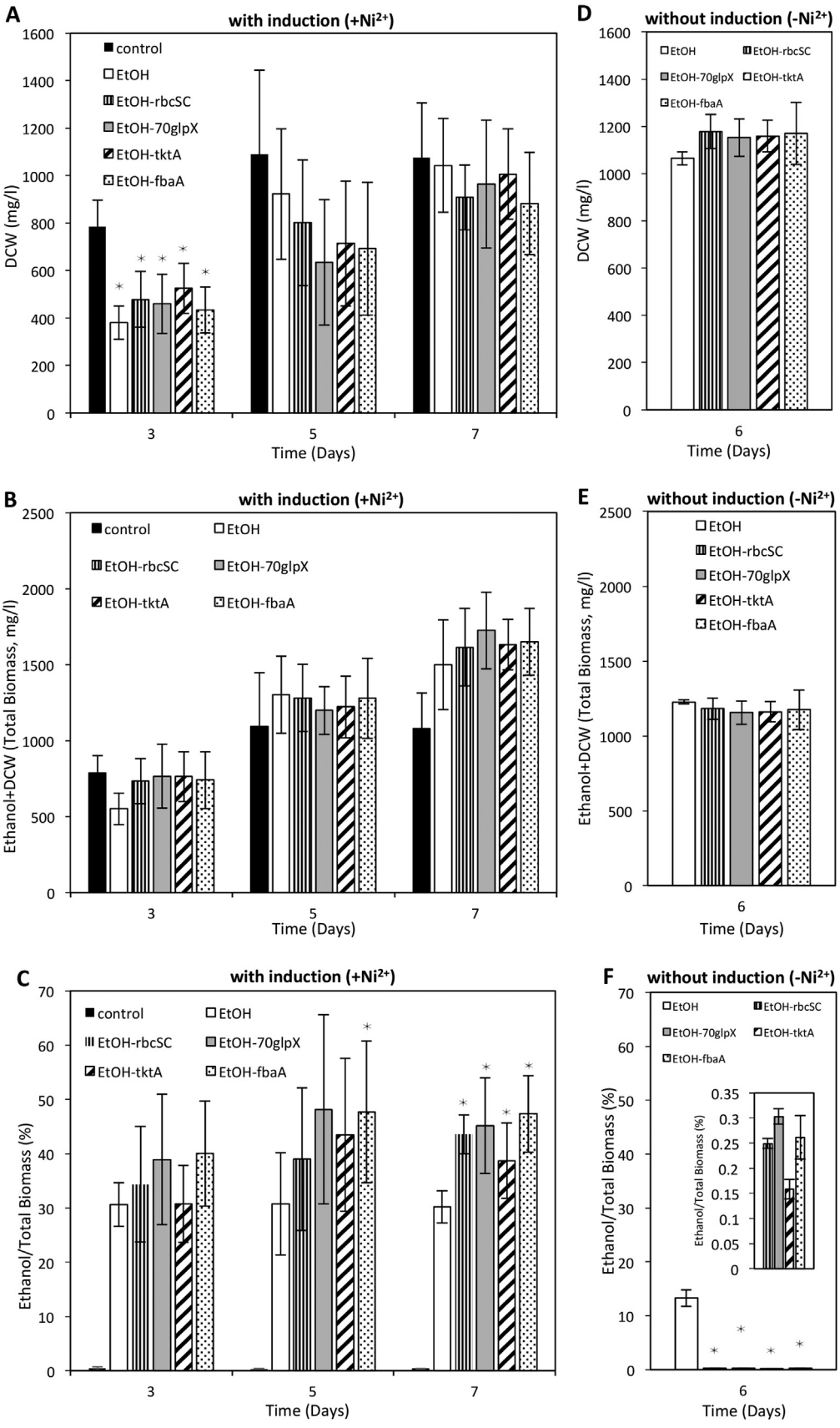

Fig. 4. Dry cell weight (DCW), total biomass (DCW + ethanol), and ethanol to total biomass ratio of cells cultivated with 50 mM $NaHCO_3$ and under 65 µmol photons m^{-2} s^{-1} light intensity with (A, B and C) and without (D, E and F) 2.5 µM Ni^{2+} induction. Error bars represent standard deviations, in A, B and C from six biological replicates conducted in three independent experiments, and in D, E and F from biological triplicates. One-way ANOVA analysis was applied. Asterisks in figure A indicate significant differences ($P < 0.05$) between control and ethanol producing strains. Asterisks in others indicate significant differences ($P < 0.05$) between strains with the ethanol synthesis pathway alone and with one of the CBB genes co-overexpressed. The insert in figure F shows the same data at a different scale. For strain information see Table 1.

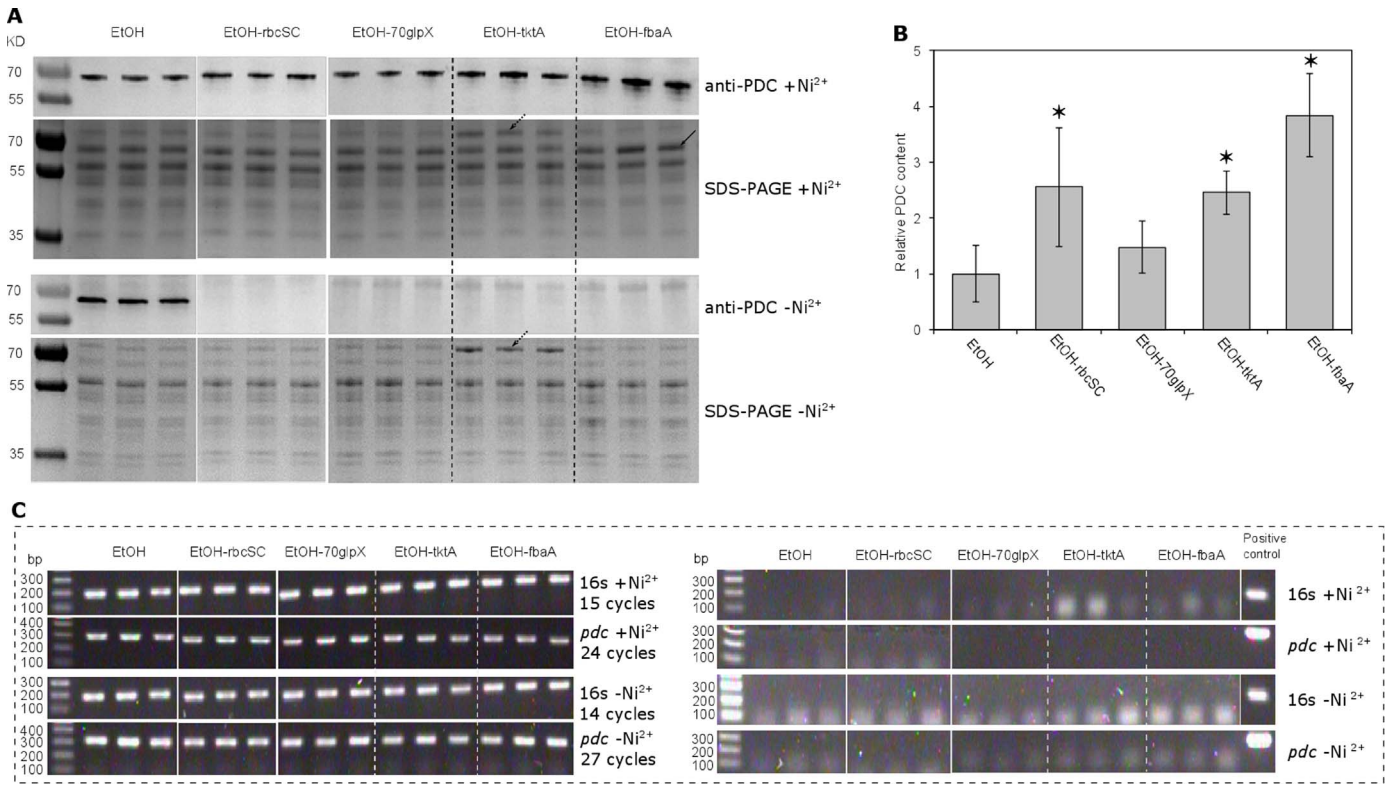

Fig. 5. Pyruvate decarboxylase (PDC) protein and mRNA content. Cells were cultivated with 50 mM $NaHCO_3$ and under 65 µmol photons m^{-2} s^{-1} light intensity. A, Western immunoblotting using a anti-PDC antibody (top panel, 1 µg crude protein), Coomassie staining SDS-PAGE (top middle panel, 5 µg crude protein) of extracts from cells grown with 2.5 µM Ni^{2+} (+Ni^{2+}), Western immunoblotting using an anti-PDC antibody (lower middle panel, 5 µg crude protein), and Coomassie staining SDS-PAGE (lower panel, 5 µg crude protein) of extracts from cells grown without addition of Ni^{2+} (-Ni^{2+}). The solid arrow indicates the PDC band on the SDS-PAGE gel, while the dotted arrows indicate the TK band. B, Relative PDC content of strains EtOH, EtOH-rbcSC, EtOH-70glpX, EtOH-tktA and EtOH-fbaA calculated with Quantity-one software. Error bars represent standard deviations from biological triplication and technical replication. One-way ANOVA analysis was applied. Asterisks indicate significant differences ($P < 0.05$) between strains with the ethanol synthesis pathway alone and with one of the CBB genes co-overexpressed. C, PDC mRNA content based on RT-PCR. On the left, upper panel and middle upper panel show samples from cells grown with 2.5 µM Ni^{2+} (+Ni^{2+}). 500 ng RNA was used to synthesize cDNA and 1 µl dsDNA was loaded. Middle lower panel and lower panel show samples from cells grown without addition of Ni^{2+} (-Ni^{2+}). 1 µg RNA was used to synthesize cDNA and 1 µl dsDNA was loaded. On the right, is the negative control for all samples showing that the RNA used for cDNA synthesis was free of DNA contamination. *Synechocystis* genomic DNA was used as template for 16S positive control, while pEtOH was used for the *pdc* positive control. For strain information see Table 1.

generation. There was no clear difference in abundance of *pdc* mRNA between the strain only expressing ethanol synthesis cassette and the strains with one of the four selected CBB cycle genes co-overexpressed (Fig. 5C). When cells were not induced, *pdc* mRNA could be detected after 27 cycles based on 1 µg total RNA as starting material. Again, no clear difference was detected between the ethanol producing strains (Fig. 5C). This indicates that Ni^{2+} induction increased the transcription level of *pdc* as expected and consistent with previous studies (Englund et al., 2016). Taking ethanol production and mRNA content of strains without induction into consideration together, failure to detect PDC on Western immunoblotting of the non-induced co-overexpression strains (Fig. 5A) may be due to the PDC protein being below the detection level.

3.3. Enhanced ethanol production in cyanobacterial cells grown at low light

Our previous studies showed that overexpressing one of the four selected CBB genes did not have positive effects on cell growth under low light intensity (15 µmol photons m^{-2} s^{-1}). However, the maximum oxygen evolution rate increased (Liang and Lindblad, 2016). This suggested some positive effect on the photosystem II water splitting activity. In this study, ethanol production was determined under this cultivation condition to examine if it would give similar results as growth. The strain expressing the ethanol synthesis cassette alone (EtOH) was the reference strain. Strains with both ethanol synthesis cassette and one of the four selected CBB cycle genes overexpressed (EtOH-rbcSC, EtOH-70glpX, EtOH-tktA, and EtOH-fbaA) were compared with the reference strain. The growth of EtOH, EtOH-rbcSC, EtOH-70glpX, EtOH-tktA and EtOH-fbaA were not significantly different between each other, both with and without P*nrsB* induced (Fig. 6A and B).

Ethanol production in strains with one of the four selected CBB cycle genes co-overexpressed with ethanol synthesis cassette was higher than that of the reference strain when P*nrsB* was induced. All the strains reached the highest production on day 7, and the ethanol production in EtOH-rbcSC was increased by 36%, EtOH-70glpX by 39%, EtOH-tktA by 38% and in EtOH-fbaA by 55% compared to EtOH (Fig. 6C). When P*nrsB* was not induced, ethanol production in strains with the CBB cycle enzymes co-overexpressed was much lower than the strain only expressing the ethanol synthesis pathway, similar to the effects when cells were cultivated under 65 µmol photons m^{-2} s^{-1} with 50 mM $NaHCO_3$ and without induction (Fig. 3D). However, under 15 µmol photons m^{-2} s^{-1} and without induction, ethanol production of strains with one of the CBB cycle genes overexpressed could be 82% (EtOH-70glpX on day 3) of that from EtOH, proportionally much higher than that when cell grown under 65 µmol protons m^{-2} s^{-1} light intensity (2%). The detected production titers (around 10 mg/l, Fig. 6D) were also higher than that in the corresponding cultures at 65 µmol photons m^{-2} s^{-1} (less than 3.5 mg/l, Fig. 3D), even though the cultivation under 65 µmol photons m^{-2} s^{-1} was conducted in sealed flasks. As cultures became dense, ethanol production of EtOH-rbcSC, EtOH-70glpX, EtOH-tktA and EtOH-fbaA remained less than half of that in EtOH, except EtOH-fbaA on day 7 that was 58% (Fig. 6D).

Introducing one of the CBB cycle genes did not show positive effect

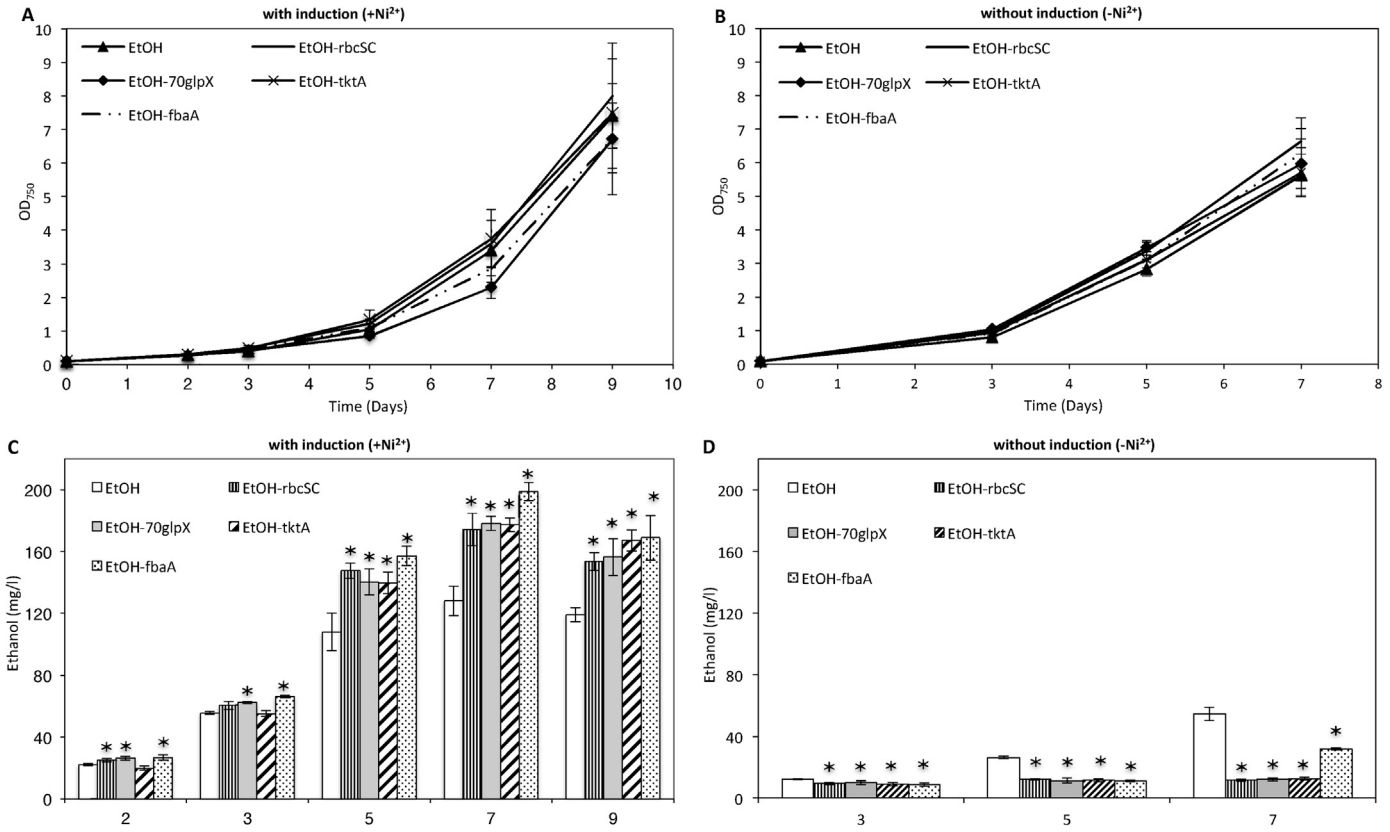

Fig. 6. Growth curves (A and B) and ethanol yield (C and D). Cells were cultivated under 15 μmol photons m^{-2} s^{-1} light intensity with (A and C) and without (B and D) 2.5 μM Ni^{2+} induction. Error bars represent standard deviation from biological triplicates. One-way ANOVA analysis was applied. Asterisks indicate significant differences ($P < 0.05$) between strains with the ethanol synthesis pathway alone and with one of the CBB genes co-overexpressed.

on growth under low light conditions (Fig. 6A and B) which was consistent with what we detected before (Liang and Lindblad, 2016). However, this engineering had positive effects on ethanol production under the same growth condition (Fig. 6C). The positive effects were consistent with the results that cells showed enhanced maximum oxygen evolution rates under this growth condition (Liang and Lindblad, 2016).

4. Discussion

The CBB cycle is the main pathway that converts atmospheric CO_2 into carbon skeletons. In this study, an ethanol synthesis pathway, consisting of PDC and ADH, alone or together with one of the four CBB cycles proteins, RuBisCO, FBA, FBP/SBPase or TK, were introduced into *Synechocystis*. The results showed that introducing an effective carbon sink, the induced ethanol synthesis pathway (with expression driven by the inducible P*nrsB*), increased the total biomass (ethanol plus dry cell weight) accumulation (Fig. 4B), which is consistent with results from *Synechococcus elongatus* PCC 7942 with sucrose secretion. The engineered *Synechococcus elongatus* PCC 7942 strain showed an increased biomass accumulation rate and photosystem II activity due to the efficient sucrose synthesis and excretion ability (Abramson et al., 2016; Ducat et al., 2012). The present study further showed that increasing the levels of one of the four selected CBB cycle enzymes resulted in even higher total biomass (Fig. 4B). In the early growth stage, ethanol producing had strong effects on DCW (Fig. 4A). This is consistent with the growth curves (Fig. 3C). This may be explained by the light availability per cell. At the beginning of the cultivation, when the cultures were relatively diluted, available light per cell is sufficient. For the control strain, it used energy and carbons to build up the cells since there was no other possible sink, or output. However, the ethanol-producing strains may maintain the basic cell survival and direct energy and carbon (pyruvate) to the extra sink, ethanol. As result, the DCW of ethanol producing strains were significantly lower than in the control strain at the beginning of the growth period. Overall, overexpressing the CBB cycles genes increased the total biomass accumulation, mainly by increasing the production of ethanol instead of growth (OD_{750} and DCW) when the ethanol synthesis pathway was efficiently expressed.

As contrast, when the carbon sink was not functioning efficiently (P*nrsB* without induction in this study), overexpressing the CBB cycle genes had severe negative effect on ethanol production (Figs. 3D and 6D). As demonstrated before, introducing one of the CBB cycle enzymes would increase the biomass accumulation under 65 μmol photons m^{-2} s^{-1} or higher light intensity (Liang and Lindblad, 2016, 2017). Consistent with this, positive effects on DCW were observed here (Fig. 4D). However, ethanol production was not increased, since one of its synthesis enzymes PDC was too low in the co-overexpressed strains (Fig. 5A), which acted as the main limitation in ethanol synthesis here. The reason why the PDC protein in the strains with one of the CBB cycle enzymes co-overexpressed was at undetectable levels is not clear. However, it was found that the levels of PDC varied between different strains (Fig. 5A and B), in a manner corresponding with the ethanol production (Fig. 3C and D). Combining the results of ethanol and total biomass production under different induction conditions show that when there was PDC present in the cells, it directs pyruvate to ethanol formation which results in less biomass accumulation but more total biomass (Fig. 4A and B). In contrast, when there was no PDC present, the cells accumulated more biomass but not more total biomass (Fig. 4D and E). Therefore, PDC plays a critical role at locating the carbons to ethanol or other cell components, measured as DCW at the end.

It has been reported that the compositional context can affect gene expression, via supercoiling as well as promoter structure, ribosome binding sites etc. (Yeung et al., 2016). In the present study, the *pdc* mRNA levels were determined in cells with or without induction

(Fig. 6C) in order to confirm that the differences on protein levels and the subsequent ethanol yield were not due to differences in transcription. There were no obvious differences of *pdc* mRNA levels between strains with ethanol synthesis pathway expressed alone and with one of the four selected CBB genes co-overexpressed (Fig. 5C), indicating similar transcription levels in different strains.

In the present study, a plasmid expression platform was used. One of the shortages to use a plasmid expression is that the corresponding antibiotic is always required to maintain the genetic construct in the cells. However, the expression on the plasmid used here was higher than when inserted into the genome (Ng et al., 2015). One explanation for this is the higher copy number of the RSF1010 derived plasmids than the genome (Ng et al., 2000). For further studies and potential industrial applications, inserting the target genes into the genome and using antibiotic free constructs may be required, in order to keep the strains genetically stable without any selection pressure.

Conclusively, the first step to increase biofuel yield should be to eliminate bottlenecks in the synthesis pathway. Afterwards, other strategies like increasing carbon fixation or optimizing growth conditions may be applied. The present study demonstrates that overexpressing one of the four-selected CBB cycle genes enhanced the production of an introduced capacity to produce a biofuel, a sink, exemplified with ethanol, when the biofuel synthesis pathway is not the main bottleneck. The results showed similar effects on the ethanol production from different CBB cycle enzymes overexpressed. In fact, under certain conditions, several enzymes combined control the flux, while one enzyme may play the main role. We hypothesize that having one enzyme overexpressed will shift the limit to another enzyme. Future research may address balanced expression levels of the CBB cycle enzymes.

Acknowledgements

Antibodies against PDC from *Zymononas mobilis* were kindly provided by Dr. Lonnie Ingram (University of Florida, USA). This work was supported by a Chinese scholarship to Feiyan Liang (201304910361) from The Chinese Service Center for Scholarly Exchange, the Swedish Energy Agency (grant # 38334-1), and the NordForsk NCoE program “NordAqua” (project # 82845).

References

Abramson, B.W., Kachel, B., Kramer, D.M., Ducat, D.C., 2016. Increased photochemical efficiency in cyanobacteria via an engineered sucrose sink. Plant Cell Physiol. 57 (12), 2451–2460. http://dx.doi.org/10.1093/pcp/pcw169.

Aldrich, H.C., McDowell, L., Barbosa, M.D.F.S., Yomano, L.P., Scopes, R.K., Ingram, L.O., 1992. Immunocytochemical localization of glycolytic and fermentative enzymes in *Zymomonas mobilis*. J. Bacteriol. 174 (13), 4504–4508.

Antonovsky, N., Gleizer, S., Noor, E., Zohar, Y., Herz, E., Barenholz, U., Milo, R., 2016. Sugar synthesis from CO_2 in *Escherichia coli*. Cell 166 (1), 115–125. http://dx.doi.org/10.1016/j.cell.2016.05.064.

Antonovsky, N., Gleizer, S., Milo, R., 2017. Engineering carbon fixation in *E. coli*: from heterologous RuBisCO expression to the Calvin–Benson–Bassham cycle. Curr. Opin. Biotechnol. 47, 83–91. http://dx.doi.org/10.1016/j.copbio.2017.06.006.

Atsumi, S., Higashide, W., Liao, J.C., 2009. Direct photosynthetic recycling of carbon dioxide to isobutyraldehyde. Nat. Biotechnol. 27 (12), 1177–1180. http://dx.doi.org/10.1038/nbt.1586.

Dejtisakdi, W., Miller, S.M., 2016. Overexpression of Calvin cycle enzyme fructose 1,6-bisphosphatase in *Chlamydomonas reinhardtii* has a detrimental effect on growth. Algal Res. 14, 116–126. http://dx.doi.org/10.1016/j.algal.2016.01.003.

Ducat, D.C., Avelar-Rivas, J.A., Way, J.C., Silvera, P.A., 2012. Rerouting carbon flux to enhance photosynthetic productivity. Appl. Environ. Microbiol. 78 (8), 2660–2668. http://dx.doi.org/10.1128/AEM.07901-11.

Englund, E., Liang, F., Lindberg, P., 2016. Evaluation of promoters and ribosome binding sites for biotechnological applications in the unicellular cyanobacterium *Synechocystis* sp. PCC 6803. Sci. Rep. 6 (1), 36640. http://dx.doi.org/10.1038/srep36640.

Erb, T.J., Jones, P.R., Bar-Even, A., 2017. Synthetic metabolism: metabolic engineering meets enzyme design. Curr. Opin. Chem. Biol. 37, 56–62. http://dx.doi.org/10.1016/j.cbpa.2016.12.023.

Feng, L., Wang, K., Li, Y., Tan, Y., Kong, J., Li, H., Zhu, Y., 2007. Overexpression of SBPase enhances photosynthesis against high temperature stress in transgenic rice plants. Plant Cell Rep. 26 (9), 1635–1646. http://dx.doi.org/10.1007/s00299-006-0299-y.

Gao, Z., Zhao, H., Li, Z., Tan, X., Lu, X., 2012. Photosynthetic production of ethanol from carbon dioxide in genetically engineered cyanobacteria. Energy Environ. Sci. 5 (12), 9857–9865. http://dx.doi.org/10.1039/C2EE22675H.

Greene, D.N., Whitney, S.M., Matsumura, I., 2007. Artificially evolved *Synechococcus* PCC6301 Rubisco variants exhibit improvements in folding and catalytic efficiency. Biochem. J. 404 (3), 517–524. http://dx.doi.org/10.1042/BJ20070071.

Henkes, S., Sonnewald, U., Badur, R., Flachmann, R., Stitt, M., 2001. A small decrease of plastid transketolase activity in antisense tobacco transformants has dramatic effects on photosynthesis and phenylpropanoid metabolism. Plant Cell 13, 535–551. http://dx.doi.org/10.1105/tpc.13.3.535.

Huang, H.H., Camsund, D., Lindblad, P., Heidorn, T., 2010. Design and characterization of molecular tools for a synthetic biology approach towards developing cyanobacterial biotechnology. Nucleic Acids Res. 38 (8), 2577–2593. http://dx.doi.org/10.1093/nar/gkq164.

Iwaki, T., Haranoh, K., Inoue, N., Kojima, K., Satoh, R., Nishino, T., Wadano, A., 2006. Expression of foreign type I ribulose-1,5-bisphosphate carboxylase/ oxygenase (EC 4.1.1.39) stimulates photosynthesis in cyanobacterium *Synechococcus* PCC7942 cells. Photosynth. Res. 88 (3), 287–297. http://dx.doi.org/10.1007/s11120-006-9048-x.

Kanno, M., Carroll, A.L., Atsumi, S., 2017. Global metabolic rewiring for improved CO_2 fixation and chemical production in cyanobacteria. Nat. Commun. 8, 14724. http://dx.doi.org/10.1038/ncomms14724.

Khozaei, M., Fisk, S., Lawson, T., Gibon, Y., Sulpice, R., Stitt, M., Raines, C.A., 2015. Overexpression of plastid transketolase in tobacco results in a thiamine auxotrophic phenotype. Plant Cell Online 27 (2), 432–447. http://dx.doi.org/10.1105/tpc.114.131011.

Köhler, I.H., Ruiz-Vera, U.M., VanLoocke, A., Thomey, M.L., Clemente, T., Long, S.P., Bernacchi, C.J., 2017. Expression of cyanobacterial FBP/SBPase in soybean prevents yield depression under future climate conditions. J. Exp. Bot. 68 (3), 715–726. http://dx.doi.org/10.1093/jxb/erw435.

Lai, M.C., Lan, E.I., 2015. Advances in metabolic engineering of cyanobacteria for photosynthetic biochemical production. Metabolites 5 (4), 636–658. http://dx.doi.org/10.3390/metabo5040636.

Li, Y.-J., Wang, M.-M., Chen, Y.-W., Wang, M., Fan, L.-H., Tan, T.-W., 2017. Engineered yeast with a CO_2-fixation pathway to improve the bio-ethanol production from xylose-mixed sugars. Sci. Rep. 7, 43875. http://dx.doi.org/10.1038/srep43875.

Liang, F., Lindblad, P., 2016. Effects of overexpressing photosynthetic carbon flux control enzymes in the cyanobacterium *Synechocystis* PCC 6803. Metab. Eng. 38, 56–64. http://dx.doi.org/10.1016/j.ymben.2016.06.005.

Liang, F., Lindblad, P., 2017. *Synechocystis* PCC 6803 overexpressing RuBisCO grow faster with increased photosynthesis. Metab. Eng. Commun. 4, 29–36. http://dx.doi.org/10.1016/j.meteno.2017.02.002.

Lin, M.T., Occhialini, A., Andralojc, P.J., Parry, M.A.J., Hanson, M.R., 2014. A faster Rubisco with potential to increase photosynthesis in crops. Nature 513 (7519), 547–550. http://dx.doi.org/10.1038/nature13776.

Ma, W., Shi, D., Wang, Q., Wei, L., Chen, H., 2005. Exogenous expression of the wheat chloroplastic fructose-1,6-bisphosphatase gene enhances photosynthesis in the transgenic cyanobacterium, *Anabaena* PCC7120. J. Appl. Phycol. 17 (3), 273–280. http://dx.doi.org/10.1007/s10811-005-4850-y.

Marraccini, P., Bulteau, S., Cassier-Chauvat, C., Mermet-Bouvier, P., Chauvat, F., 1993. A conjugative plasmid vector for promoter analysis in several cyanobacteria of the genera *Synechococcus* and *Synechocystis*. Plant Mol. Biol. 23 (4), 905–909. http://dx.doi.org/10.1007/BF00021546.

Miao, R., Wegelius, A., Durall, C., Liang, F., Khanna, N., Lindblad, P., 2017. Engineering cyanobacteria for biofuel production. In: Hallenbeck, P. (Ed.), Modern Topics in the Phototrophic Prokaryotes: Environmental and Applied Aspects. Springer International Publishing, Switzerland, pp. 351–393. http://dx.doi.org/10.1007/978-3-319-46261-5_11.

Miyagawa, Y., Tamoi, M., Shigeoka, S., 2001. Overexpression of a cyanobacterial fructose-1,6-/sedoheptulose-1,7-bisphosphatase in tobacco enhances photosynthesis and growth. Nat. Biotechnol. 19, 965–969. http://dx.doi.org/10.1038/nbt1001-965.

Ng, A.H., Berla, B.M., Pakrasi, H.B., 2015. Fine-tuning of photoautotrophic protein production by combining promoters and neutral sites in the cyanobacterium *Synechocystis* sp. strains PCC 6803. Appl. Environ. Microbiol. 81 (19), 6857–6863. http://dx.doi.org/10.1128/AEM.01349-15.

Ng, W.O., Zentella, R., Wang, Y., Taylor, J.S., Pakrasi, H.B., 2000. PhrA, the major photoreactivating factor in the cyanobacterium *Synechocystis* sp. strain PCC 6803 codes for a cyclobutane-pyrimidine-dimer-specific DNA photolyase. Arch. Microbiol. 173 (5–6), 412–417. http://dx.doi.org/10.1007/s002030000164.

Occhialini, A., Lin, M.T., Andralojc, P.J., Hanson, M.R., Parry, M.A.J., 2016. Transgenic tobacco plants with improved cyanobacterial Rubisco expression but no extra assembly factors grow at near wild-type rates if provided with elevated CO_2. Plant J. 85 (1), 148–160. http://dx.doi.org/10.1111/tpj.13098.

Ogawa, T., Tamoi, M., Kimura, A., Mine, A., Sakuyama, H., Yoshida, E., Shigeoka, S., 2015. Enhancement of photosynthetic capacity in Euglena gracilis by expression of cyanobacterial fructose-1,6-/sedoheptulose-1,7-bisphosphatase leads to increases in biomass and wax ester production. Biotechnol. Biofuels 8 (1), 80. http://dx.doi.org/10.1186/s13068-015-0264-5.

Park, J., Choi, Y., 2017. Cofactor engineering in cyanobacteria to overcome imbalance between NADPH and NADH: a mini review. Front. Chem. Sci. Eng. 11 (1), 66–71. http://dx.doi.org/10.1007/s11705-016-1591-1.

Raines, C.A., 2003. The calvin cycle revisited. Photosynth. Res. 75 (1), 1–10. http://dx.doi.org/10.1023/A:1022421515027.

Rosenthal, D.M., Locke, A.M., Khozaei, M., Raines, C.A., Long, S.P., Ort, D.R., 2011. Overexpressing the C3 photosynthesis cycle enzyme sedoheptulose-1-7 bisphosphatase improves photosynthetic carbon gain and yield under fully open air CO_2 fumigation

(FACE). BMC Plant Biol. 11 (1), 123. http://dx.doi.org/10.1186/1471-2229-11-123.
Ruffing, A.M., 2014. Improved free fatty acid production in Cyanobacteria with *Synechococcus* sp. PCC 7002 as host. Front. Bioeng. Biotechnol. 2, 1–10. http://dx.doi.org/10.3389/fbioe.2014.00017.
Savir, Y., Noor, E., Milo, R., Tlusty, T., 2010. Cross-species analysis traces adaptation of Rubisco toward optimality in a low-dimensional landscape. Proc. Natl. Acad. Sci. USA 107 (8), 3475–3480. http://dx.doi.org/10.1073/pnas.0911663107.
Simkin, A.J., Lopez-Calcagno, P.E., Davey, P.A., Headland, L.R., Lawson, T., Timm, S., Raines, C.A., 2017. Simultaneous stimulation of sedoheptulose 1,7-bisphosphatase, fructose 1,6-bisphophate aldolase and the photorespiratory glycine decarboxylase-H protein increases CO_2 assimilation, vegetative biomass and seed yield in *Arabidopsis*. Plant Biotechnol. J. 15 (7), 805–816. http://dx.doi.org/10.1111/pbi.12676.
Stanier, R.Y., Kunisawa, R., Mandel, M., Cohen-Bazire, G., 1971. Purification and properties of unicellular blue-green algae (order Chroococcales). Bacteriol. Rev. 35 (2), 171–205. http://dx.doi.org/10.1016/j.jbiotec.2013.07.020.
Tamoi, M., Takeda, T., Shigeoka, S., 1999. Functional analysis of fructose-1,6-bisphosphatase isozymes (fbp-I and fbp-II gene products) in Cyanobacteria. Plant Cell Physiol. 40 (2), 257–261.
Uematsu, K., Suzuki, N., Iwamae, T., Inui, M., Yukawa, H., 2012. Increased fructose 1,6-bisphosphate aldolase in plastids enhances growth and photosynthesis of tobacco plants. J. Exp. Bot. 63 (8), 3001–3009. http://dx.doi.org/10.1093/jxb/ers004.
Whitney, S.M., Birch, R., Kelso, C., Beck, J.L., Kapralov, M.V., 2015. Improving recombinant Rubisco biogenesis, plant photosynthesis and growth by coexpressing its ancillary RAF1 chaperone. Proc. Natl. Acad. Sci. USA 112 (11), 3564–3569. http://dx.doi.org/10.1073/pnas.1420536112.
Yeung, E., Dy, A.J., Martin, K.B., Ng, A.H., Vecchio, D. Del, Beck, J.L., James, J., 2016. The effect of compositional context on synthetic gene net- works. bioRxiv 1–35.
Zhu, X.-G., de Sturler, E., Long, S.P., 2007. Optimizing the distribution of resources between enzymes of carbon metabolism can dramatically increase photosynthetic rate: a numerical simulation using an evolutionary algorithm. Plant Physiol. 145 (2), 513–526. http://dx.doi.org/10.1104/pp.107.103713.